Resonant optical rectification in bacteriorhodopsin

Géza I. Groma*, Anne Colonna†, Jean-Christophe Lambry†, Jacob W. Petrich†‡, György Váró*, Manuel Joffre†, Marten H. Vos†§, and Jean-Louis Martin†

*Institute of Biophysics, Biological Research Centre of the Hungarian Academy of Sciences, Szeged, H-6726, Hungary; †Laboratory for Optical Biosciences, Instute National de la Santé et de la Recherche Médicale U451, Centre National de la Recherche Scientifique, Unité Mixte de Recherche 7645, Ecole Polytechnique–Ecole Nationale Supérieure de Techniques Avancées, 91128 Palaiseau Cedex, France; and ‡Department of Chemistry, Iowa State University, Ames, IA 50011

Edited by Mostafa A. El-Sayed, Georgia Institute of Technology, Atlanta, GA, and approved March 25, 2004 (received for review October 21, 2003)

The relative role of retinal isomerization and microscopic polarization in the phototransduction process of bacteriorhodopsin is still an open question. It is known that both processes occur on an ultrafast time scale. The retinal trans→cis photoisomerization takes place on the time scale of a few hundred femtoseconds. On the other hand, it has been proposed that the primary light-induced event is a sudden polarization of the retinal environment, although there is no direct experimental evidence for femtosecond charge displacements, because photovoltaic techniques cannot be used to detect charge movements faster than picoseconds. Making use of the known high second-order susceptibility $\chi^{(2)}$ of retinal in proteins, we have used a nonlinear technique, interferometric detection of coherent infrared emission, to study macroscopically oriented bacteriorhodopsin-containing purple membranes. We report and characterize impulsive macroscopic polarization of these films by optical rectification of an 11-fs visible light pulse in resonance with the optical transition. This finding provides direct evidence for charge separation as a precursor event for subsequent functional processes. A simple two-level model incorporating the resonant second-order optical properties of retinal, which are known to be a requirement for functioning of bacteriorhodopsin, is used to describe the observations. In addition to the electronic response, long-lived infrared emission at specific frequencies was observed, reflecting charge movements associated with vibrational motions. The simultaneous and phase-sensitive observation of both the electronic and vibrational signals opens the way to study the transduction of the initial polarization into structural dynamics.

Retinal proteins play an essential role in a broad range of light-driven biological processes, including vision (1), energy transduction (2), and circadian control (3). All these functions involve both the conversion of light energy into charge separation and retinal isomerization, but the interplay of these processes is the subject of intense debate. The retinal protein of which the initial photochemistry is most extensively studied is the photosynthetic protein bacteriorhodopsin (bR). This protein colors the purple membrane of halobacteria and acts as a light-driven proton pump by means of a multistep process termed the photocycle (2). In the traditional model for the initial transduction step in this cycle is directly light-driven trans→cis isomerization of retinal (4–6); this model has been recently extended by including excited-state skeletal stretching (5, 7). However, experiments with modified bR containing nonisomerizable retinal analogs challenged this model by showing that the initial photo-induced events are not associated with retinal isomerization (8–10). In fact, in an early alternative hypothesis (11), the essential process was proposed to be dielectric relaxation of the protein as a response to sudden polarization upon retinal excitation (11–13). Recent molecular dynamics calculations (14) and experiments (15, 16) support this view.

Direct measurements of this charge separation process by using photovoltaic techniques have been performed (17–19). However, the intrinsic temporal resolution of these techniques is limited to several picoseconds; i.e., slower than the ≈500-fs (4, 20) isomerization process. To visualize the electronic response of bR on a time scale that is limited only by the laser pulse length, we introduce a different approach, exploiting a nonlinear technique: interferometric detection of optical rectification. The second order susceptibility $\chi^{(2)}$ of the retinal chromophore is unusually high, especially in its native protein environment, and this property has been shown to be a requirement for functioning of bR (21). These strong nonlinear characteristics have been demonstrated in (off-resonance) frequency up-conversion ($\omega \rightarrow 2\omega$) experiments (22–25). The same property should also give rise to functionally more relevant frequency down-conversion ($\omega \rightarrow 0$) or optical rectification (26). This phenomenon has been observed in noncentrosymmetric semiconductors (27–30) and organic crystals (31) in the form of single-cycle radiation in the THz and midinfrared region as a response to ultrashort laser pulses but not in biological materials. On the other hand, long-lasting coherent infrared emission has been observed from heme protein crystals (32), originating solely from the vibrational response of the protein. Here, we report impulsive macroscopic polarization of oriented bR films by optical rectification of an 11-fs visible light pulse in resonance with the optical transition, providing a direct evidence for charge separation as a precursor event for subsequent functional processes.

Materials and Methods

bR-containing purple membranes were prepared from strain S9 of *Halobacterium salinarium* by standard methods (33). An outline of the experimental arrangement is depicted in Fig. 1. Oriented bR films were deposited and dried on germanium plates by using an electrophoretic method, described for deposition on titanium-oxide covered glass in ref. 34. For our experiments, germanium was chosen as a substrate, because it is transparent in the infrared, and, at the same time, its conductance is high enough to act as an electrode during electrophoretic deposition. The optical density of the films of ≈2,000 membrane layers (thickness ≈ 10 μm) is ≈2 at the 565-nm visible absorption maximum. In these films, the retinal chromophores are oriented at ≈28° with respect to the plane (35–37), and the two-dimensional orientation in the plane is random.

The experimental setup (32) was based on a noncollinear optical parametric amplifier (NOPA) pumped by a titanium-sapphire regenerative amplifier and delivering ≈11-fs pulses centered at 560 nm (near the maximum of bR absorption) at 1 kHz. The NOPA output was split, and one part (≈75 nJ, subsequently attenuated to avoid damage) was used to excite the sample by focusing to ≈50 μm directly on the side of the sample where the bR film was deposited. The angle α between the sample and the plane perpendicular to the beams was variable, and the sample could be continuously rotated (≈6 Hz, diameter ≈ 1 cm) in the plane of films so that the excitation volume was

This paper was submitted directly (Track II) to the PNAS office.

Abbreviations: bR, bacteriorhodopsin; GaAs, gallium arsenide.

§To whom correspondence should be addressed. E-mail: marten.vos@polytechnique.fr.

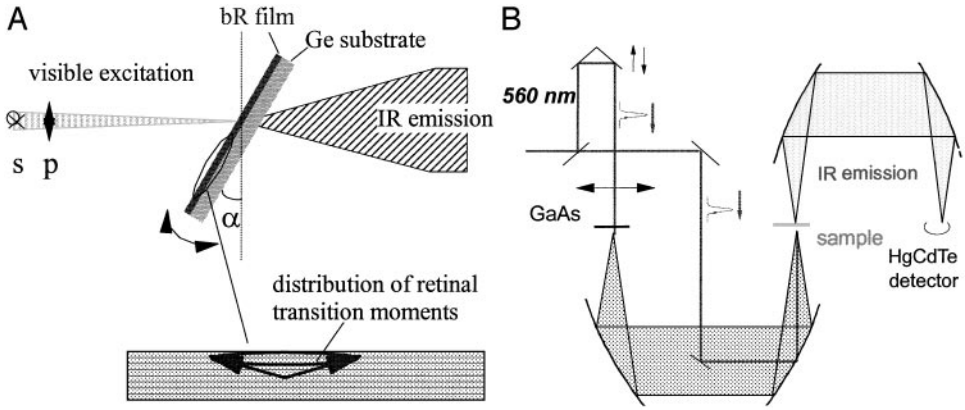

Fig. 1. Experimental arrangement for emission generation in bR films. (*A*) Positioning of the bR films with respect to the visible excitation beam. (*B*) Scheme of the interferometric arrangement for characterizing the radiation emitted from the bR films. See text for details.

renewed between shots. IR emission in the forward direction, passing through the Ge substrate, was focused on a HgCdTe detector (low-frequency cut-off ≈700 cm^{-1}). Another part of the NOPA output was used to generate an IR reference beam, by optical rectification in a gallium arsenide (GaAs) crystal (type $<1\,\bar{1}\,0>$, thickness 110 μm) (28). This beam was also focused on the detector and spatially overlapped with the IR emission beam from the sample. Polarization (s or p) of the visible beam and the reference beams was variable. An interferogram was constructed by varying the delay of the two visible pulses.

Results and Discussion

The experiment is based on coherent, interferometric detection of the infrared emission (28, 32, 38) generated in dried oriented bR films, by means of interference with a reference emission originating from a GaAs crystal, which is a well known source of optical rectification. Unlike the previous second harmonic generation measurements on bR (22–25), which were conducted off-resonance and did not provide any temporal information on the polarization, this experiment was carried out at full resonance and with ≈11-fs time resolution. Fig. 2*A* shows an interferogram resulting from the coherent IR emission of a bR film and compares it with a similar experiment with a second GaAs crystal at the sample position. The bR–GaAs interferogram is dominated by a strong signal around $t = 0$, very similar to that observed in the GaAs–GaAs experiment. Thus, most of the emission is instantaneous broadband IR, typical for electronic optical rectification. In the time domain, such an emission consists of a single cycle; the appearance of the symmetric ringing in the experimental interferogram is due to the steep low frequency cut-off of the detector (28). In addition, in the bR–GaAs experiment, a small asymmetric (only at $t > 0$) complex oscillatory feature is observed that extends beyond 1.3 ps and is not present in the GaAs–GaAs optical rectification. This signal and the corresponding modulation of the Fourier transform spectrum (Fig. 2*B*) presumably reflects the IR-active vibrational response of the retinal-protein system and is equivalent to the effect we have observed previously in myoglobin crystals (32). We stress, however, that an equivalent of the main, broadband emission signal has not been observed on myoglobin (32); this is, therefore, a previously uncharacterized example of electronic optical rectification in a biological sample.

The amplitude of the bR signal is comparable to that of GaAs. At $\alpha = 45°$ (see below) and by using ≈15% of the available visible excitation energy to avoid damage on bR, the signal amounted to ≈10% of the GaAs signal. With a rotating film, the signal is linear with the excitation intensity (Fig. 3*A*). Because the measured signal is the emitted electric field strength, this implies that the intensity of the emission is quadratic with excitation intensity, as expected for a $\chi^{(2)}$ process. With immobile films at higher intensities, the signal appears somewhat nonlinear in excitation intensity (data not shown). We ascribe this effect to a greater penetration depth in the bR film of the visible excitation pulse at higher intensities, leading to a diminished net attenuation by the film of the emitted beam.

The symmetry axis of the system is perpendicular to the film; hence, the resultant light-induced electric polarization takes place in this direction. Consequently in a second-order process, the emitted beam is polarized with a component in the direction

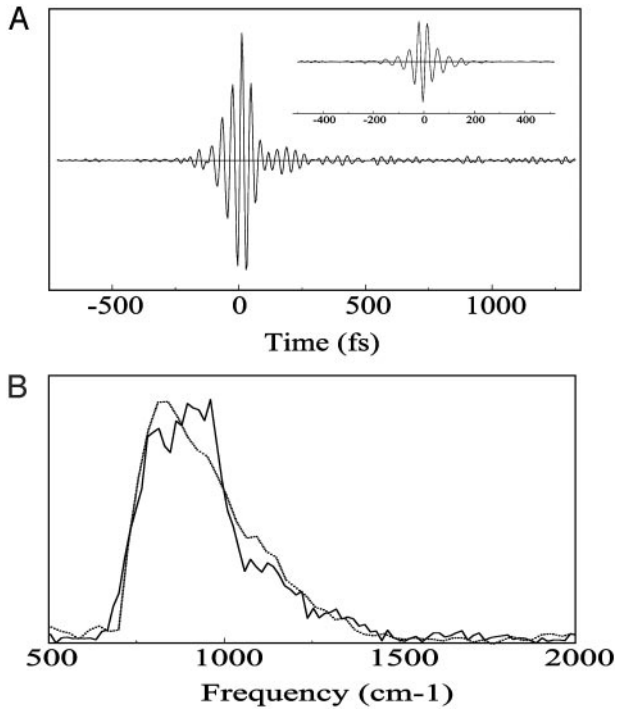

Fig. 2. (*A*) Interferogram of emission from bR and the reference pulse (α = 45°) taken with a rotating bR film so that subsequent pulses excite new volumes. (*Inset*) Interferogram with a GaAs crystal at the position of the sample and the bR film placed in front of the detector to take its filtering effect into account. Here, the signal was corrected for a small pump-induced long-lived transmission change observed in GaAs (≈5% of the maximal signal). (*B*) Fourier transform of the interferogram of the bR film (solid trace) and the GaAs-reference experiment (dotted trace).

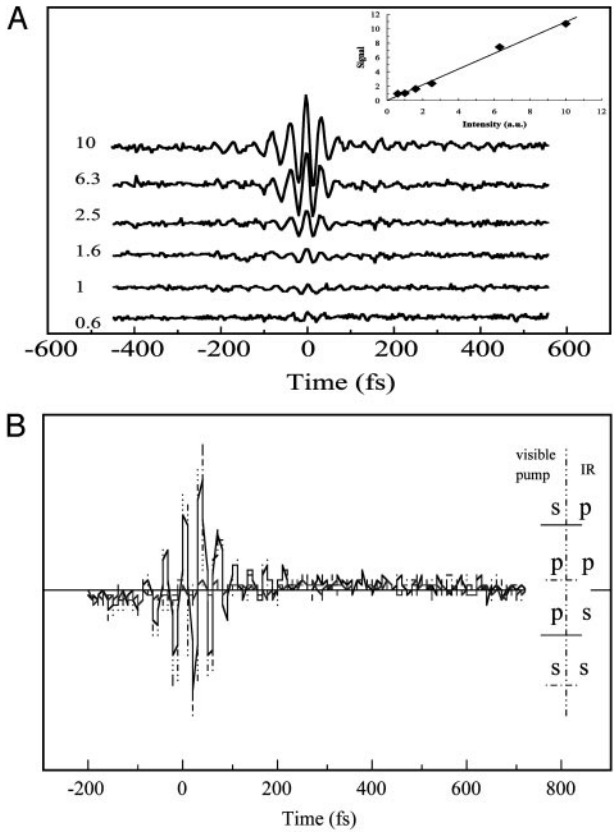

Fig. 3. (*A*) Interferograms at various intensities of the pump beam with rotating films. (*Inset*) Signal amplitudes. (*B*) Polarization (see Fig. 1) dependence of the signal. The polarization of the pump beam and that of the reference beam were varied independently. An IR polarizer was placed in front of the detector in the direction of the polarization of the reference beam.

of the symmetry axis, and its intensity is zero in this direction. Accordingly, the signal was only observed when the film was tilted with respect to the plane perpendicular to the optical axis (see Fig. 1); the signal maximum was found at $\alpha \approx 45°$. Fig. 3*B* shows that the emitted signal is always polarized in the direction of the projection of the symmetry axis of the system onto the plane perpendicular to the optical axis, independent of the polarization of the incident beam. Altogether, the dependence of the signal on the experimental geometry is fully consistent with a second order nonlinear origin, as expected for optical rectification.

Fig. 3*B* also shows that the intensity of the emitted IR beam is roughly similar for s and p polarization of the incident visible beam. To understand this finding, it should be realized that the experiment was conducted under resonant and strongly absorbing conditions (virtually all photons are absorbed by the film). In this case, it is the component of the molecular second-order polarizability tensor in the direction normal to the film that contributes to the macroscopic emission. Assuming this polarizability has a major component in the direction of the retinal (23), these contributions are similar for all absorbing molecules. We emphasize that different conditions apply in the transparent, off-resonance regime, as illustrated by the observed strong polarization dependence of frequency doubling of 1,064-nm light in bR films by Lewis and coworkers (23).

Theoretical Treatment. The second-order polarization $P^{(2)}(r,t)$ of a single, isolated molecule as a response to the electric field $E(r,t)$ of the exciting light is characterized by the second-order response function $S^{(2)}(t_2,t_1)$ according to

$$P^{(2)}(r,t) = \int_0^\infty dt_2 \int_0^\infty dt_1 S^{(2)}(t_2,t_1)\mathrm{E}(r,t-t_2)\mathrm{E}(r,t-t_2-t_1)\,. \qquad [1]$$

In the case of noninteracting molecules, the frequency domain counterpart of $S^{(2)}(t_2,t_1)$ is proportional to $\chi^{(2)}$. We applied the method of Liouville-space pathways (39) with a complete T_1 relaxation matrix (40) to derive a simple but sufficiently general formula for the response function (G.G, M.J., M.H.V., and J.-L.M., unpublished results). $S^{(2)}(t_2,t_1)$ can be partitioned into second harmonic and optical rectification terms. The former reproduces the formula of Oudar and Chemla (41) in the special case of off-resonance. The calculation of $S^{(2)}t_2,t_1$ using the method of Liouville-space pathways also reproduces results obtained from the Bloch equation for a two- or three-level system (38). For a laser pulse described by $E(t) = Env(t)\cos(\omega t)$, the optical rectification term is formally equivalent to the above general expression for the second order polarization if the complete electric field is substituted by its envelope:

$$P^{(2)}_{OR}(t) = \int_0^\infty dt_2 \int_0^\infty dt_1 S_0{}^{(2)}(t_2,t_1)Env(t-t_2)Env(t-t_2-t_1)\,. \qquad [2]$$

For a two-level system and keeping only resonant terms, we find

$$S^{(2)}_0(t_2,t_1) \sim \mu^2_{10}\Delta\mu e^{-\left(\frac{t_2}{T_1}+\frac{t_1}{T_2}\right)}\cos((\omega-\omega_{10})t_1)\,, \qquad [3]$$

where ω_{10} and μ_{10} are the transition frequency and dipole moment, respectively, $\Delta\mu$ is the difference of the dipole moment between the two states, whereas T_1 and T_2 are the familiar population and phase relaxation times, respectively.

According to the above model, if the excitation is fully resonant, the evolution of the polarization is identical to that of the excited state population. This situation was not analyzed earlier, notwithstanding its importance for the primary function of bR. In a classical view, upon absorption of a photon, the system undergoes an instantaneous polarization proportional to $\Delta\mu$, decays together with the population of the excited state, and, therefore, acts as an ultrafast diode. The applied theory thus connects the concept of sudden polarization and the resonant optical rectification.

In the present experiment, we monitored the above polarization change by detecting the radiation emitted by the dipole. For a single molecule, the elementary effect is a Hertzian dipole radiation, resulting in a signal proportional to the second time derivative of the dipole moment. [For the real excitation geometry, this approaches the first derivative (29)]. The used technique visualizes the derivative corresponding to the rising part. We emphasize that in this model the polarization itself remains after decay of the electronic coherent emission signal. Extension of this technique to the THz regime may allow observation of the subsequent evolution of the excited state polarization and, in addition, may connect with the earlier photovoltaic measurements with lower time resolution (17, 19).

Unfortunately, comparison of oriented bR samples with GaAs does not directly allow the quantification of the dipole moment

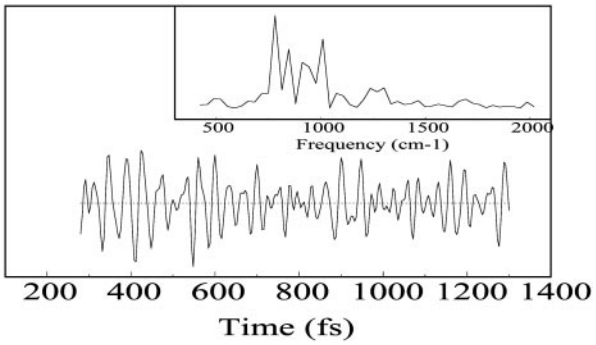

Fig. 4. Vibrational part of the interferogram of Fig. 1 and Fourier transform power spectrum.

change $\overrightarrow{\Delta\mu}$ measured in our experiments because the relevant nonlinear response of GaAs is not straightforwardly accessible. Indeed, the strong absorption of GaAs in the visible region makes the nonlinear propagation equation difficult to solve considering both the complicated dynamics of the generated free carriers and the reshaping of the incident pulse because of the strong frequency dependence of the absorption coefficient. An exploration of other reference materials may help to address this issue. More detailed comparison with a well characterized reference will in addition allow to separate any contributions from the chromophore and protein electronic response to the initial polarization in the 100-fs time range (see below).

Oscillatory Features. The oscillatory features following the electronic polarization response display major frequency components particularly in the 700–1,000 cm^{-1} range (Fig. 4). Vibrations in this range have been observed in transient absorption experiments (42, 43), and they correspond predominantly to the hydrogen-out-of-plane vibrational modes of the retinal. The present result that they are detectable in coherent emission experiments implies that they are associated with charge displacements in the transmembrane direction, indicating that the initial polarization specifically sets in motion these modes. As a preliminary analysis, we have performed a gliding window Fourier transform analysis that indicates a modulation of the frequency of the hydrogen-out-of-plane modes (*cf.* ref. 43) and persistence of these motions beyond retinal isomerization.

The vibrational features are significantly different when the bR film is continuously rotated in the plane of the membrane during data acquisition, so as to renew the sample volume between laser pulses, compared with the case when the film is immobile (the data shown in Figs. 2, 3*A*, and 4 are taken with rotating films). The shape of the main broadband emission signal, associated to the optical rectification process, does not change upon moving the film. We assign these differences to accumulation of photocycle intermediates in the case of kHz excitation of an immobile film. In particular, the photocycle has been shown to be particularly slow in dried films and completed only in the ≈100-ms time range (44).

Concluding Remarks. Molecular dynamics calculations (14) and recent photon echo experiments (16) indicate that optical excitation of the retinal is followed by an intense dielectric response of the protein matrix in the 100-fs range. Our experiments show that the initial electronic polarization precedes this response, which suggests that the polarization induces the large electrostatic protein relaxation (16). Studies on bR samples reconstituted with nonisomerizable retinal (15) showed that retinal isomerization is not a prerequisite for conformational changes to occur in the protein on the microsecond time scale. However, required for the bR photocycle are large nonlinear susceptibilities of the retinal (21) and, therewith, the capability to perform optical rectification. The applied theory of second-order optics connects the concepts of optical rectification to the original idea of sudden polarization. The inherent noncentrosymmetric structure of the membrane makes possible the primary and instantaneous conversion of light energy into electrical polarization by this nonlinear effect. The experiments presented here directly time-resolve this functionally important polarization and indicate that they are at the origin of specific vibrational motions involving charge displacements.

J.W.P. thanks the Ecole Polytechnique and Iowa State University for support during sabbatical leave. This work was supported by Országos Tudományos Kutatási Alapprogramok (OTKA) Grant T 029 878 and the ULTRA (Femtochemistry and Femtobiology) Program of the European Science Foundation.

1. Pepe, I. M. (2001) *Prog. Ret. Eye Res.* **20,** 733–759.
2. Lanyi, J. K. (1999) *Int. Rev. Cytol.* **187,** 161–202.
3. Provenchio, I., Rodriguez, I. R., Jiang, G., Hayes, W. P., Moreira, E. F. & Rollag, M. D. (2000) *J. Neurosci.* **20,** 600–605.
4. Mathies, R. A., Brito Cruz, C. H., Pollard, W. T. & Shank, C. V. (1988) *Science* **240,** 777–779.
5. Garavelli, M., Negri, F. & Olivucci, M. (1999) *J. Am. Chem. Soc.* **121,** 1023–1029.
6. Warshel, A. & Chu, Z. T. (2001) *J. Phys. Chem.* **105,** 9857–9871.
7. Song, L. & El-Sayed, M. A. (1998) *J. Am. Chem. Soc.* **120,** 8889–8890.
8. Zhong, Q., Ruhman, S., Ottolenghi, M., Sheves, M., Friedman, N., Atkinson, G. H. & Delaney, J. K. (1996) *J. Am. Chem. Soc.* **118,** 12828–12829.
9. Rousso, I., Khachatryan, E., Gat, Y., Brodsky, I., Ottolenghi, M., Sheves, M. & Lewis, A. (1997) *Proc. Natl. Acad. Sci. USA* **94,** 7937–7941.
10. Ye, T., Friedman, N., Gat, Y., Atkinson, G. H., Sheves, M., Ottolenghi, M. & Ruhman, S. (1999) *J. Phys. Chem.* **103,** 5122–5130.
11. Lewis, A. (1978) *Proc. Natl. Acad. Sci. USA* **75,** 549–553.
12. Mathies, R. & Stryer, L. (1976) *Proc. Natl. Acad. Sci. USA* **73,** 2169–2173.
13. Birge, R. R. & Zhang, C. F. (1990) *J. Chem. Phys.* **92,** 7178–7195.
14. Xu, D., Martin, C. & Schulten, K. (1996) *Biophys. J.* **70,** 453–460.
15. Aharoni, A., Hou, B., Friedman, N., Ottolenghi, M., Rousso, I., Ruhman, S., Sheves, M., Ye, T. & Zhong, Q. (2001) *Biochemistry (Moscow)* **66,** 1210–1219.
16. Kennis, J. T. M., Larsen, D. S., Ohta, K., Facciotti, M., Glaeser, R. M. & Fleming, G. R. (2002) *J. Phys. Chem. B* **106,** 6067–6080.
17. Groma, G. I., Szabó, G. & Váró, G. (1984) *Nature* **308,** 557–558.
18. Groma, G. I., Hebling, J., Ludwig, C. & Kuhl, J. (1995) *Biophys. J.* **69,** 2060–2065.
19. Xu, J., Stickrath, A. B., Bhattacharya, P., Nees, J., Varo, G., Hillebrecht, J. R., Ren, L. & Birge, R. R. (2003) *Biophys. J.* **85,** 1128–1134.
20. Herbst, J., Heyne, K. & Diller, R. (2002) *Science* **297,** 822–825.
21. Zadok, U., Khatchatouriants, A., Lewis, A., Ottolenghi, M. & Sheves, M. (2002) *J. Am. Chem. Soc.* **124,** 11844–11845.
22. Aktsipetrov, O. A., Akhmediev, N. N., Vsevolodov, N. N., Esikov, D. A. & Shutov, D. A. (1987) *Sov. Phys. Dokl.* **32,** 219–220.
23. Huang, J., Chen, Z. & Lewis, A. (1989) *J. Phys. Chem.* **93,** 3314–3320.
24. Huang, J., Lewis, A. & Rasing, T. (1988) *J. Phys. Chem.* **92,** 1756–1759.
25. Song, Q., Wan, C. & Johnson, C. K. (1994) *J. Phys. Chem.* **98,** 1999–2001.
26. Shen, Y. R. (1984) *The Principles of Nonlinear Optics* (Wiley, New York).
27. Auston, D. H., Cheung, K. P., Valdmanis, J. A. & Kleinman, D. A. (1984) *Phys. Rev. Lett.* **53,** 1555–1558.
28. Bonvalet, A., Joffre, M., Martin, J.-L. & Migus, A. (1995) *Appl. Phys. Lett.* **67,** 2907–2909.
29. Bonvalet, A. & Joffre, M. (1998) in *Femtosecond Laser Pulses*, ed. Rullière, C. (Springer, Berlin), pp. 285–305.
30. Huber, R., Brodschelm, A., Tauser, F. & Leitenstorfer, A. (2000) *Appl. Phys. Lett.* **76,** 3191–3193.
31. Carey, J. J., Bailey, R. T., Pugh, D., Sherwood, J. N., Cruickshank, F. R. & Wynne, K. (2002) *Appl. Phys. Lett.* **81,** 4335–4337.
32. Groot, M.-L., Vos, M. H., Schlichting, I., van Mourik, F., Joffre, M., Lambry, J.-C. & Martin, J.-L. (2002) *Proc. Natl. Acad. Sci. USA* **99,** 1323–1328.
33. Oesterhelt, D. & Stoeckenius, W. (1974) *Methods Enzymol.* **31,** 667–678.
34. Varo, G. & Keszthelyi, L. (1983) *Biophys. J.* **43,** 47–51.
35. Heyn, M. P., Cherry, R. J. & Müller, U. (1977) *J. Mol. Biol.* **117,** 607–620.
36. Huang, J. Y. & Lewis, A. (1989) *Biophys. J.* **55,** 835–842.

37. Hudson, B. S. & Birge, R. R. (1999) *J. Phys. Chem.* **103,** 2274–2281.
38. Bonvalet, A., Nagle, J., Berger, V., Migus, A., Martin, J.-L. & Joffre, M. (1996) *Phys. Rev. Lett.* **76,** 4392–4395.
39. Mukamel, S. (1995) *Principles of Nonlinear Optical Spectroscopy* (Oxford Univ. Press, Oxford).
40. Boyd, R. W. & Mukamel, S. (1984) *Phys. Rev. A At. Mol. Opt. Phys.* **29,** 1973–1983.
41. Oudar, J. L. & Chemla, D. S. (1977) *J. Chem. Phys.* **66,** 2664–2668.
42. Dexheimer, S. L., Wang, Q., Peteanu, L. A., Pollard, W. T., Mathies, R. A. & Shank, C. V. (1992) *Chem. Phys. Lett.* **188,** 61–66.
43. Kobayashi, T., Saito, T. & Ohtani, H. (2001) *Nature* **414,** 531–534.
44. Groma, G. I., Kelemen, L., Kulcsar, A., Lakatos, M. & Varo, G. (2001) *Biophys. J.* **81,** 3432–3441.